J Stat Phys (2009) 137: 717–727
DOI 10.1007/s10955-009-9860-8

Depinning of a Discrete Elastic String from a Random Array of Weak Pinning Points with Finite Dimensions

Laurent Proville

Received: 12 June 2009 / Accepted: 26 October 2009 / Published online: 12 November 2009

Abstract In possible connection with dislocation pinning by foreign atoms in alloys and vortex pinning in type II superconductors, we compute the external force required to drag an elastic string along a discrete two-dimensional random array with finite dimensions. The obstacles, with a maximum pinning force f_m are distributed randomly on a rectangular lattice with square symmetry. The system dimensions are fixed by the total course of the elastic string L_x and the string length L_y. Our study shows that Larkin's length is larger than L_y when f_m is less than a certain bound depending on the system size as well as on the obstacle density c_s. Below such a bound an analytical theory is developed to compute the depinning threshold. Some numerical simulations allow us to demonstrate the accuracy of the theory for an obstacle density ranging from 1 to 50% and for different geometries.

Keywords Depinning transition · Dislocation · Solid solution hardening · Vortex

1 Introduction

Within analytical theories for dislocation depinning [13–15, 17, 25, 30–32, 43], the dislocation was thought of as a continuous elastic string impinged on a two-dimensional (2D) random static potential. The depinning transition in such a model is a typical issue of statistical physics, belonging to a broad class of problems concerned with extended interfaces motion in heterogeneous media [4–8, 10, 12, 21, 22, 26, 29, 33, 41, 44, 47, 49, 50]. From the dimensional analysis of vortices pinning in superconductors, Larkin et al. derived a typical length [3, 27] given by $\mathcal{L}_c \sim a(\Gamma/\bar{f}\sqrt{c_s})^{2/3}$, where a is the shortest interatomic distance, $\bar{f}$ is a typical pinning force that characterizes the string-obstacle interaction, c_s is the atomic density of obstacles and Γ corresponds to the elastic line tension. Larkin's length fixes the size of the domains where the pinning on disorder is stronger than elastic forces. The difference between both competing effects fixes a finite depinning threshold above which the elastic interface starts gliding. From the previous formula, it is seen that $\mathcal{L}_c$ increases as the

L. Proville (✉)
CEA, DEN Service de Recherches de Métallurgie Physique, 91191 Gif-sur-Yvette, France
e-mail: lproville@cea.fr

ratio $\Gamma/\bar{f}$ increases and that by extrapolation, Larkin's length may even pass the total string length, i.e., in the cases of stiff strings anchored by very weak pinning points. Such a situation may present some interest in regard of different physical problems. In solid solutions the dislocations are anchored by atom-sized obstacles that impede the plastic flow thereby yielding solid solution hardening [11]. Then the maximum pinning force of the foreign atoms is of few hundredth nano-Newton [9, 28, 35, 37, 39, 40, 45, 46] while the dislocation line tension ranges around several nano-Newton in deformed metals with typical dislocation density $\rho_d = 10^{12}$ m^{-2}. According to the linear elastic theory of dislocations [20] such a line tension varies as $\ln(1/\rho_d)$, leading to stiffer dislocations in materials with less extended defects. In monocrystalline alloys with short dislocations as in thin folds, one can therefore expect $\mathcal{L}_c$ being larger than the dislocation length. The second physical problem where diverging $\mathcal{L}_c$ could occur is type II superconductors where the vortices pinning forces [2, 36] and line tension [18, 42] may have same orders as for dislocations in solid solutions. The similarities in depinning transition of vortices and dislocations triggered Labusch's work in both fields [23, 24]. However, the peculiarity of vortices in superconductors hinges on a pinning force which would vanish at the temperature of the superconducting phase transition T_c, as shown experimentally in Niobium [36]. Then the closer from T_c the smaller the ratio $\Gamma/\bar{f}$ which leads, as for dislocations in materials with small ρ_d, to a Larkin's length that diverges. In the limit of a stiff string and weak pinning, another expectation from Larkin's model concerns the wandering W which would vary as the inverse of the ratio $\Gamma/\bar{f}$. A physical lower bound for W is the unit cell of the lattice bearing obstacles, typically the shortest interatomic distance in solids.

In the present paper, the depinning of an elastic string is studied in situations where $\mathcal{L}_c$ is larger than the total string length and W is of the order of the shortest distance between lattice sites. To approach such a problem, the continuous version of the elastic string model is replaced with a discrete spring chain the nodes of which move on a 2D square lattice and interact with pinning points randomly distributed on lattice sites. This very simple model allows us to devise an analytical theory which accounts for the discreteness of the obstacle distribution and the finite dimensions of the system. In order to demonstrate the accuracy of the theory, the latter is compared with simulations. Theory and numerical computations agree remarkably well for a broad range of model parameters, e.g., (i) the in-plane obstacle density c_s, (ii) the lattice size in every direction of space, (iii) the maximum pinning force f_m and (iv) the potential interaction cutoff w. The theoretical predictions proves reliable on the condition that f_m and w remain smaller than certain bounds varying with c_s and lattice dimensions.

The paper is organized as follows. In Sect. 2, the spring chain model is introduced and the numerical computations are described. In Sect. 3, the statistical theory is derived and compared with numerical data. The results are resumed and commented in Sect. 4.

2 The Discrete String Model

An elastic string is discretized with a spatial step b, equivalent to the shortest interatomic distance in solids. Each node of the discrete chain is bound to its first neighbor by an harmonic spring of strength Γ. The two quantities, b and Γ are chosen to scale distances and forces, respectively. The size of the lattice in the direction of the chain is denoted as L_y whereas the distance over which the chain is dragged is L_x. The spring chain nodes move along the X-axis while Y-axis points in the main line direction. The 2D random array of obstacles is constructed by selecting randomly the occupied lattice sites, up to a number

of obstacle equals to $c_s L_x L_y$, where c_s is the obstacle density. Since the depinning process occurs when chain nodes pass the obstacle force maximum, the interaction potential is expended as a polynomial function in the vicinity of such a maximum. Assuming that the interaction is attractive and that the potential is symmetric with respect to its minimum, we obtain a polynomial function of fourth order:

$$\begin{aligned} V(x) &= V_0(x^2/w^2 - 1)^2 \quad \text{for } |x| < w, \\ V(x) &= 0 \quad \text{for } |x| > w, \end{aligned} \tag{1}$$

which corresponds to a force maximum $f_m = 8|V_0|/(3\sqrt{3}w)$, attained when $x = \pm w/\sqrt{3}$. The chain nodes interact solely with obstacles situated in the column along which they may glide. The parameter w fixes how the interaction decreases in the vicinity of the force maximum f_m. Both f_m and w can be extracted from atomistic data as those reported in [37, 39].

The dimensionless over-damped Langevin dynamics for the chain node k is given by:

$$\dot{x_k} = [x_{k+1} + x_{k-1} - 2x_k] + \tau - \sum_i 4V_0 \frac{(x_k - s_{k,i})}{w^2} \left(\frac{(x_k - s_{k,i})^2}{w^2} - 1 \right), \tag{2}$$

where x_k is the position of the node k, τ is the external force and $s_{k,i}$ is the coordinate of the ith obstacle in the kth row. For the weak pinning forces we are concerned with, the chain strain remains very small such that the anharmonic terms in the spring tension have been neglected. Properly scaled, the continuous version of the spring chain model served in the development of the solid solution hardening theory [15, 17, 24, 30, 32]. It also belongs to the wide class of elastic interface models, extensively studied in statistical physics [4, 8, 12, 26, 33, 41, 44, 47].

In the course of the numerical integration for Eq. 2, τ is incremented adiabatically. Once $[\sup_k |\dot{x_k}|]$ is inferior to a certain precision (i.e., 10^{-7}) the external force is incremented. Before each increment, the chain configuration is recorded and once the chain has run over a distance L_x, the integration is stopped. The latest anchored configuration corresponds to the strongest one and the associated external force is denoted as τ_c, i.e., the static depinning threshold. We performed this type of simulations for different lattice aspect ratios, varying L_x and L_y and for different obstacle densities ranging from 1 to 50%.

In Fig. 1(a), we report the strongest chain configuration, obtained from the numerical simulations for a pinning strength $f_m = 0.1$. The critical profile is found to wander and to cross at least 40 lattice rows. In Fig. 1(b), the critical chain profile is shown for smaller values of f_m, i.e., two orders of magnitude smaller than the one used in Fig. 1(a). We note that the entire string length is bounded by only two lattice rows. The simulations evidence actually a well known feature for pinning of extended defects [26], namely weaker the obstacles flatter the shape of the critical configuration. A perfectly rigid string would even experience a null force since then V_0 would be negligible in Eq. 2. However, as soon as some elasticity enters into play, τ_c is finite. The case of wavy critical profile as seen from Fig. 1(a) has been studied extensively in the past, both through numerical simulations [1, 16, 19, 34, 48] and analytical works [14, 24]. The predictions drawn from the theories on depinning of wavy profiles can be expected to be inadequate for systems with quasi-straight critical profile, since the string wandering is then inferior or of the order of the inter-atomic spacing. Then a discrete approach is required. The present work is essentially concerned with cases like the one presented in Fig. 1(b), where the elastic string shape is quasi-straight.

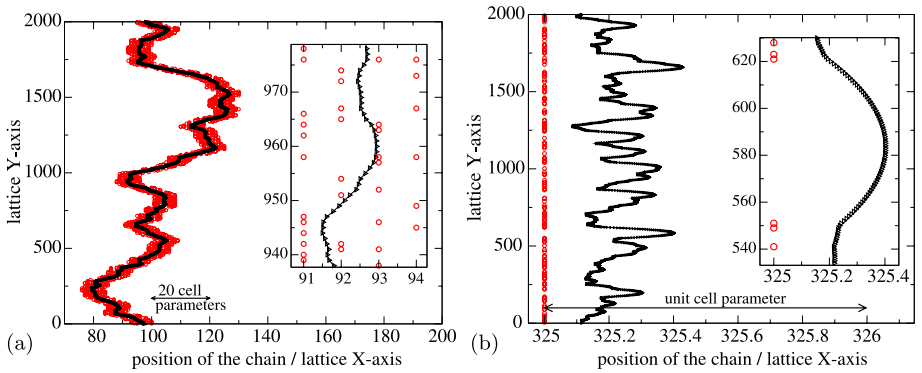

Fig. 1 (**a**) Strongest pinning configuration of the spring chain on a random array of obstacles (*circles*) for $f_m = 0.1$, $L_y = 2000$, $L_x = 500$, a density $c_s = 16\%$ and an interaction cutoff $w = 1$. Only obstacles close from the chain have been reported for clarity. *Inset* shows a magnification of obstacles (*circles*) and nodes (*triangles*) of the chain segment. X and Y axis have different scaling for convenience of the plot. (**b**) Same as in (**a**) but for $w = 0.5$, $f_m = 0.005$ and the obstacle density $c_s = 7\%$

3 Vacant Site Cluster Sampling Theory

In the insets shown in Fig. 1(b), it is worth noticing that along the rows that bound the spring chain, some holes appear in the obstacle distributions. Hereafter, we dubbed such holes *vacant site clusters*. The statistics of such density fluctuations along lattice rows plays a key role in the determination of the maximum drag force. In Fig. 1(b), the more strongly pinned configuration remains tightly bound to a single lattice row situated at the back of the chain. The string can then be viewed as quasi-straight, notwithstanding the bulges formed between rows. When $w \leq 0.5$, we can assume that the chain interacts with rows one by one and it is natural to work on the hypothesis that for such a system the strength of the random lattice is fixed by its denser row. To convey such a remark into some algebra, one needs to study the sampling of obstacles on a finite size lattice $L_x \times L_y$. We notice that the purely random planar distribution follows Bernoulli's binomial law and that the number of obstacles N_o involved into a single row of length L_y is then a random variable which probability is given by:

$$\rho(N_o) = \mathbb{C}_{N_o}^{L_y} c_s^{N_o} (1 - c_s)^{L_y - N_o}, \tag{3}$$

where $\mathbb{C}_{N_o}^{L_y} = L_y!/N_o!(L_y - N_o)!$. Such a statistical distribution can be approximated with Poisson's law in the limit of large L_y. However such a rounding yields some error for small L_y, so we keep the binomial formulation of Eq. 3. The probability for a row to involve less than N obstacles is $\sum_{N_o<N} \rho(N_o)$ and therefore in a set of L_x rows, the probability for a row to contain N_m obstacles and $(L_x - 1)$ rows with a number of obstacles inferior to N_m is:

$$\beta(N_m) = L_x[\rho(N_m)]\left[\sum_{N_o<N_m} \rho(N_o)\right]^{L_x-1}. \tag{4}$$

The maximum number N_m fixing the number of obstacles in the denser row depends only on the lattice dimensions in each direction of space and on the overall obstacle density c_s. The mean density in the denser row is then $c_m = N_m/L_y$. When an excess of vacant sites emerges

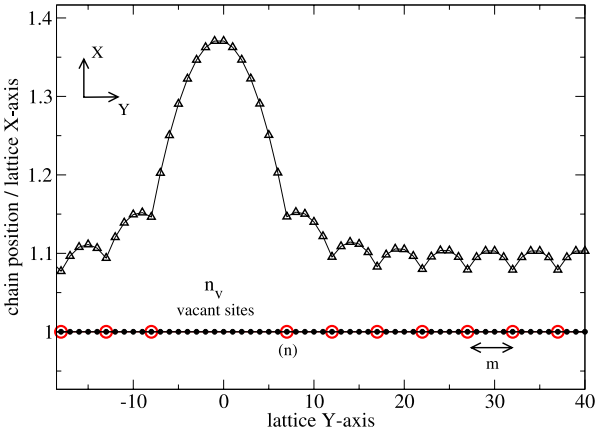

Fig. 2 Schematic representation of the model used for a quasi-straight spring chain tightly bound to a single lattice row. The *small full circles* represent the lattice sites, the *large open circles* represent the obstacles and the triangles are for the spring chain nodes. The average number n_v of vacant sites involved in the largest vacant site cluster is determined through Eqs. 6 and 5. The average spacing m between the obstacles on both sides of the largest vacant site cluster is fixed by Eq. 7

at some place along the denser row, such segment is weaker than others where the obstacles are more crowded. Thence the spring chain starts depinning on the largest vacant site clusters (VSC). The typical size of such VSC must now be determined. Actually the mean number of VSC in a row which the obstacle density is fixed to c_m is $L_{VSC} = (c_m L_y - 1) \approx N_m$. The normalized probability to find a VSC with exactly n vacant sites is $c_m(1-c_m)^n$ while the probability for a VSC which size is inferior to n is $[1-(1-c_m)^n]$. The probability to find a VSC of size n and $(L_{VSC}-1)$ VSC with size inferior to n is proportional to:

$$\gamma(n) = L_{VSC}[c_m(1-c_m)^n][1-(1-c_m)^n]^{L_{VSC}-1}. \tag{5}$$

The mean size of the largest VSC in the denser row is thus:

$$n_v = \sum_n [n\gamma(n)] / \sum_n \gamma(n). \tag{6}$$

Such a maximum VSC is surrounded by other VSCs that mean size is given by: $[\sum_{n<n_v} nc_m(1-c_m)^n]/[\sum_{n<n_v} c_m(1-c_m)^n]$ which for convenience is denoted as $(m-1)$ with:

$$m = \frac{1}{c_m} - n_v \frac{(1-c_m)^{n_v}}{1-(1-c_m)^{n_v}}. \tag{7}$$

To compute the external force associated with the strongest binding row we consider the segment of n_v vacant sites as embedded into a regular lattice of obstacles spaced by a mean distance m. Such a mean-field construction is illustrated within Fig. 2, where spring chain's nodes (triangles) are bound to the lattice sites occupied by the obstacles (large open circles). The array of obstacles is assumed to be centro-symmetric, so we ascribe the label 0 to the center of symmetry which corresponds to the top of the bulge. We also define a new variable $n = (1+n_v)/2$ for convenience of notations. Under the external applied force τ, The force balance sheet, for say the left hand side of the chain leads to the set of equations:

$$
\begin{aligned}
F_0 &= -\tau - 2(x_1 - x_0),\\
F_1 &= -\tau - (x_2 + x_0 - 2x_1),\\
F_2 &= -\tau - (x_3 + x_1 - 2x_2),\\
&. = .\\
F_{n-1} &= -\tau - (x_n + x_{n-2} - 2x_{n-1}),\\
F_n &= -\tau - f(x_n) - (x_{n+1} + x_{n-1} - 2x_n),\\
F_{n+1} &= -\tau - (x_{n+2} + x_n - 2x_{n+1}),\\
&. = .\\
F_{n+m-1} &= -\tau - (x_{n+m} + x_{n+m-2} - 2x_{n+m-1}),\\
F_{n+m} &= -\tau - f(x_{n+m}) - (x_{n+m+1} + x_{n+m-1} - 2x_{n+m}),\\
F_{n+m+1} &= -\tau - (x_{n+m+2} + x_{n+m} - 2x_{n+m+1}),
\end{aligned}
\tag{8}
$$

and in principle the series of equations repeats up to the chain boundaries with increment of subscripts. We assume that the mechanical equilibrium is satisfied for all nodes j situated in between obstacles. Then $F_j = 0$ but for $j \in [n, n+m, \ldots, n+pm]$. For the segment $j \in [0, n]$, it is easy to show by recurrence that: $x_j - x_0 = -\tau j^2/2$. For $j \in [n, n+m]$, we proceed the same and find $x_{j+n} - x_n = -\tau j(n + j/2) - [F_n + f(x_n)]j$ which fixes the segment end to

$$
x_{n+m} = x_n - \tau m(n + m/2) - m[F_n + f(x_n)]. \tag{9}
$$

The same can be iterated once again for $j \in [n+m, n+2m]$ which leads to $x_{n+2m} - x_{n+m} = -\tau m(n + 3m/2) - (F_n + F_{n+m} + f(x_n) + f(x_{n+m}))m$. The set of equation on the positions x_{n+jm} is then:

$$
\begin{aligned}
x_{n+m} &= x_n - \tau m(n + m/2) - f(x_n)m,\\
x_{n+2m} &= x_{n+m} - \tau m(n + 3m/2) - [F_n + F_{n+m} + f(x_n) + f(x_{n+m})]m,\\
&. = .\\
&. = .\\
x_{n+pm} &= x_{n+(p-1)m} - \tau m\left(n + (2p-1)\frac{m}{2}\right) - m\sum_{j=0}^{p-1}[F_{n+jm} + f(x_{n+jm})].
\end{aligned}
\tag{10}
$$

Subtracting the two latest equations yields:

$$
F_{n+pm} = -\frac{\Delta_m x_{n+pm}}{m} - \tau m - f(x_{n+pm}) \tag{11}
$$

where $\Delta_p x_{n+pm} = (x_{n+(p+1)m} + x_{n+(p-1)m} - 2x_{n+pm})$ is the discrete Laplacian applied to the p subscript. When the entire chain is at mechanical equilibrium $F_{n+pm} = 0$ for all p. Far enough from the n_v-VSC (i.e., the VSC with n_v vacant sites), the solution for x_{n+pm} tends asymptotically to a constant x_∞ such as $\tau m = -f(x_\infty)$ and therefore:

$$
x_\infty = \frac{2}{\sqrt{3}}\cos\left(\frac{\arccos(-\tau m/f_m)}{3} + \frac{4\pi}{3}\right). \tag{12}
$$

We can expend linearly Eq. 11 for the far enough sites such as the displacement x_{n+pm} writes $x_{n+pm} = x_\infty + \epsilon_p$ and $f(x_{n+pm}) = f(x_\infty) + f'(x_\infty)\epsilon_p$. Then, at the equilibrium Eq. 11 yields $[\Delta_p \epsilon_p = -f'(x_\infty) m \epsilon_p]$ and thence ϵ_p is an exponential function: $[\epsilon_p = \epsilon_0 \exp(-\alpha p)]$ which the exponent α verifies

$$\alpha = \pm 2\,\mathrm{ash}(\sqrt{-f'(x_\infty)m}/2). \tag{13}$$

Since the chain displacement is bounded, we are solely concerned with solutions such as $(\alpha p) > 0$. The sum of the whole set of equations in Eq. 10 provides another relation between τ and nodes positions x_{n+pm}, on the condition that $F_{n+pm} = 0$ for all p:

$$x_n - x_{n+pm} = m\left[\tau p(n + pm/2) + \sum_{j=0}^{p-1}(p-j) f(x_{n+jm})\right], \tag{14}$$

which after expanding $f(x_{n+jm})$ as a Taylor series around x_∞ and keeping only the terms linear in p provides us with an equation which relates τ to ϵ_0:

$$\tau = \frac{-\epsilon_0}{(n - m/2)}\left[\frac{f'(x_\infty)}{(1-e^{-\alpha})} + \frac{\epsilon_0 f''(x_\infty)}{2(1-e^{-2\alpha})} + \frac{\epsilon_0^2 f'''(x_\infty)}{6(1-e^{-3\alpha})}\right]. \tag{15}$$

The critical chain configuration is reached when the Hessian associated with Eq. 11 has a singular eigenvalue. This allows us to determine the critical value for ϵ_0. Actually we found that finding the Hessian singular eigenvalue is equivalent to find the maximum of Eq. 15 for τ with respect to ϵ_0. The solution for the critical bulge is then:

$$\epsilon_0 = -3(1-e^{-3\alpha})\frac{f''(x_\infty) - \sqrt{f''(x_\infty)^2 - 4f'''(x_\infty)f'(x_\infty)\frac{(1-e^{-2\alpha})^2}{3(1-e^{-3\alpha})(1-e^{-\alpha})}}}{2f'''(x_\infty)(1-e^{-2\alpha})}. \tag{16}$$

Combining the solutions for Eqs. 12, 13, 15 and 16 allows us to determine the maximum pinning force associated with N_m, the number of obstacle in the denser row. For this reason, we denote such a maximum as $\tau(N_m)$. The set of equations giving $\tau(N_m)$ can be solved recursively. Starting with a small enough trial solution for $\tau = \tau_0$, we compute the corresponding quantities x_∞ and α from Eq. 12 and from Eq. 13. Then ϵ_0 is derived from Eq. 16 and the corresponding value of τ from Eq. 15. If the so obtained quantity is larger than the initial value τ_0 then the latter is incremented and we proceed the same up to find identical values for τ and τ_0. The end result gives the required $\tau(N_m)$ to a precision fixed by the trial solution increment.

The maximum drag force τ_c of the random lattice is approximated by averaging $\tau(N_m)$ over N_m:

$$\tau_c = \sum_{N_m} \beta(N_m)\tau_c(N_m), \tag{17}$$

where $\beta(N_m)$ has been given in Eq. 4. The previous theory is compared to simulations data in Figs. 3(a) and (b) and in Fig. 4 for different lattice dimensions, different pinning forces, varying w and f_m. A quantitative agreement has been obtained between theory and simulations, although no adjustable parameters are involved. The theory predictions worsen for cases where the critical configuration crosses few lattice rows. From Fig. 4, it can be seen that the discrepancy increases as the density decreases while the theoretical predictions remain accurate for more concentrated obstacle distributions. As f_m increases above 0.03,

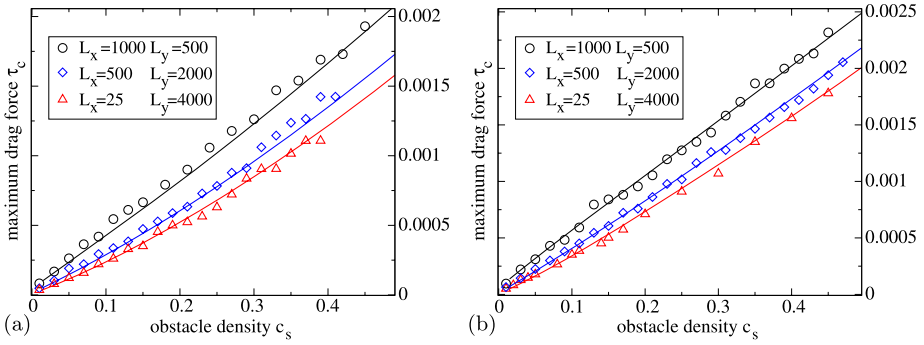

Fig. 3 External force required to drag a spring chain of length L_y over a distance L_x, for a pinning strength $f_m = 0.005$ and a cutoff $w = 0.1$ in (**a**) and $w = 0.5$ in (**b**). The *symbols* represent the data obtained through the simulations described in Sect. 2, for different lattices (see figures legend). The *continuous lines* correspond to the predictions made through the theory detailed in Sect. 3 for same parameters as those used in simulations. Colors of symbols and lines correspond one to one

the deviation between theoretical predictions and simulations data is shifted toward higher densities.

Other authors [16, 34] noticed that the depinning from a random lattice was dependant on the drag distance. Concerning the weak pinning points studied here, it is thus of some interest to explore the variation of the maximum drag force with lattice dimensions. The maximum drag force was found to vary as:

$$\tau_c \approx A(c_s, L_y)[\ln(L_x)]^{\alpha_x} \tag{18}$$

where α_x varies with all other parameters but L_x and where $A(c_s, L_y)$ is a function of c_s and L_y. For instance when $w = 0.5$, $f_m = 0.01$ and $L_y = 1000$, we found $\alpha_x = [0.018 - 0.062\ln(c_s)]$ and $A = [0.083c_s^{1.13}]$. One can thus observe that the L_x dependence is very weak since a logarithm is a rather wise function. However, strictly speaking τ_c is not bounded and increases with L_x. Actually the longer is the string course the larger is the pinning force that may be encounter along such a course.

The maximum drag force τ_c depends not only on L_x but also on L_y. It was found to vary as:

$$\tau_c \approx B_1(c_s, L_x) + \frac{B_2(c_s, L_x)}{[\ln(L_y)]^{\alpha_y}}, \tag{19}$$

where B_1 increases as a power law in c_s whereas B_2 and the logarithm exponent α_y decreases smoothly with c_s increase. For instance with $w = 0.5$, $f_m = 0.001$ and $L_x = 200$, we found $\alpha_y = [1.27 - 0.27\ln(c_s)]$, $B_1 = 9.8910^{-4}c_s^{1.41}$ and $B_2 \approx 0.003$. Extrapolating Eq. 19 to very large L_y shows that τ_c tends toward B_1, independent from L_y. The theoretical predictions for the τ_c dependence against L_y have been compared with numerical simulations in Fig. 5. The depinning threshold has been computed for different L_y and different f_m and for fixed parameters $c_s = 0.1$, $w = 0.5$ and $L_x = 200$. The numerical computations were averaged over a sampling of 15 random distributions of obstacles in order to reduce uncertainties yielded by the τ_c dispersion. As mentioned previously, the VSC theory proves accurate provided that f_m remains small enough. The upper bound on f_m for that the theory remains valid depends on other parameters, i.e., L_y, L_x, w and c_s. Figure 5 evidences the dependency on L_y for the case $f_m = 1.10^{-2}$, $w = 0.5$ and $c_s = 0.1$. Then it was found that the theory

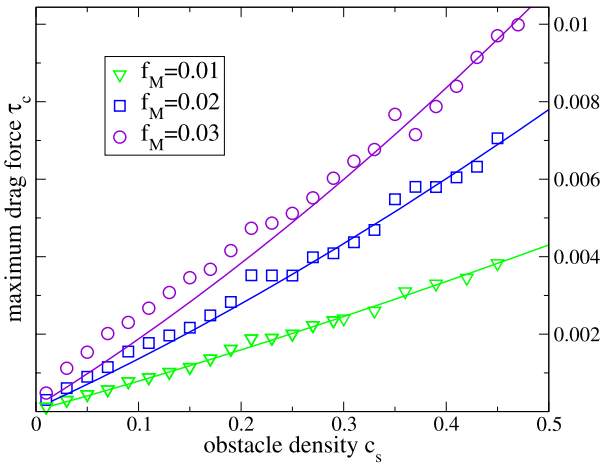

Fig. 4 External force required to drag a spring chain of length $L_y = 1000$ along a distance $L_x = 100$, for different obstacle pinning strengths (see legend) and the same interaction range $w = 0.5$. The different *symbols* represent the simulations data and the *continuous lines* correspond to the prediction made through the analytical theory detailed in the text for same parameters

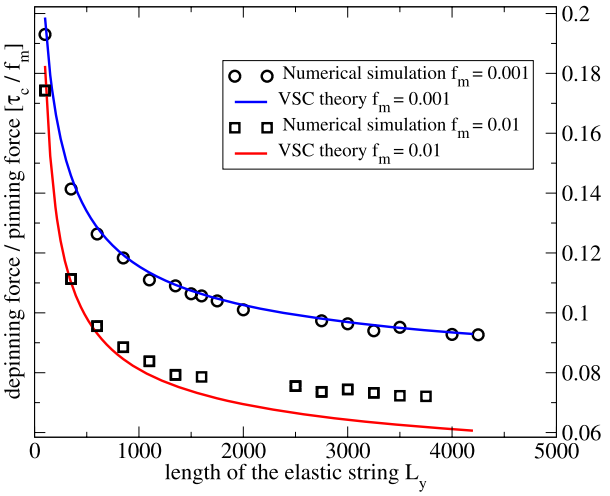

Fig. 5 Comparison between numerical computations (*symbols*) and the theory (*full lines*) for the ratio between depinning force τ_c and obstacle pinning strength f_m against the string length L_y. The drag distance is $L_x = 200$ and $f_m = 0.01$ (*squares*) or $f_m = 0.001$ (*circles*) with an interaction cutoff $w = 0.5$

is accurate for L_y smaller than $L_y^{VSC} = 1000$ while a neat departure between theory and numerics can be noticed above. We also noted that the smaller f_m the larger the bound L_y^{VSC}. As an example, in Fig. 5 for $f_m = 10^{-3}$, the theory agrees satisfactorily with simulations over the whole range of L_y which means that L_y^{VSC} is then much larger than the system dimension along the Y direction. Another point worthy to notice is that L_y^{VSC} increases with c_s and more importantly with the drag distance L_x such that for a sufficiently long course it is possible to recover the accuracy of the theory. For a finite L_y, an infinite course would actually yield a quasi-straight pinning configuration with one obstacle per site in the lattice denser row. Such a configuration corresponds to the maximal strength that could provide the disordered lattice.

From Fig. 5 it is seen that τ_c tends toward an asymptotic value as L_y takes larger values. The convergence toward a steady τ_c against L_y corresponds to the expectation drawn from Larkin's model [27] which predicts τ_c independent from L_y when the latter is much larger than $\mathcal{L}_c$ (see Sect. 1). Applying naively Larkin's model to small L_y would though lead to

erroneous predictions. For small length scales, in the energy balance sheet established by Larkin and Ovchinnikov [27], the contribution from elastic line tension is larger than the one from disorder. Then τ_c would fall to nought when L_y is less than $\mathcal{L}_c$. Usually it is said that elasticity dominate disorder on small length scales. Our computations demonstrate a neat departure from such expectation as seen from Fig. 5. When L_y is small enough, the string configuration at depinning is quasi-straight and then τ_c does not vanish but rather increases with L_y decrease. It is mainly because of the string pinning on a single lattice row that corresponds to the denser row of the disordered lattice. The present remark could be resumed into a short sentence: *Disorder dominates elasticity over all length scales*.

For fixed lattice dimensions, the adjustment of a density power law for the theoretical maximum drag force τ_c is found very close from a linear variation and may even be larger than unity in some situations depending on the lattice geometry. For instance, from Fig. 3(b), we worked out through a curve fitting with the form $\tau_c \propto (c_s^\eta)$, an exponent $\eta = 1.13$ for $L_y = 4000$ and $L_x = 25$ whereas for $L_y = 500$ and $L_x = 1000$, $\eta = 0.946$ was obtained. The effective density exponent η is therefore dependent on the dimensions of the lattice. However, such variations with respect to L_x and L_y remain weak and would be hardly identified in a narrow range of obstacle density.

4 Summary and Perspectives

A theory was derived to compute the applied force required to drag an elastic string over a disordered planar distribution of weak pinning points with finite dimensions. In comparison to numerical simulations, the theoretical predictions were found accurate provided that the critical configuration remains close from a quasi-straight line. The strongest pinning was shown to correspond to a pinning on the denser lattice rows in which the size of the vacant site clusters (VSC) is bounded in average. The maximum VSCs correspond to the weakest defects in the denser row from which the critical depinning proceeds. The mean size of the critical VSC is determined through an expression involving only lattice dimensions and the overall planar obstacle density c_s. The theory allowed us to account for the finite lattice dimensions in a quantitative manner, with no adjustable parameters. The variations of the critical applied force τ_c against the chain length L_y and the drag distance L_x are opposite: the larger L_y the smaller τ_c and the larger L_x the larger τ_c. The τ_c variation with L_y is bounded with an asymptotic value that depends on L_x and c_s. For a fixed lattice geometry, the pinning strength was found close to being linear in c_s. An extension of the VSC theory to cases with larger potential cutoff w is under progress [38]. Preliminary works demonstrate that the principal results of the present study remain.

The effects of lattice dimensions on depinning of an elastic string could be of some interest to interpret experimental works on the single vortex depinning in thin film [2] where the vortex extent is limited to several tens of nanometers, i.e., the thickness of the film. The extinction of the vortex pinning forces at the superconducting transition [36] underpins the assumption for a very weak pinning and thence for the quasi-straight critical configuration. Moreover the vortex line tension being expected to increase as the correlation length decreases [18] the vortices should be stiffer in high-T_c superconductors where the assumption of a quasi-straight critical configuration would be more amendable. Experimental works as those reported in Ref. [2] allow to measure the depinning threshold of a single vortex within a thin film of mono-crystalline cuprate, with different film thicknesses and different temperatures. According to our analysis of the data reported on the vortex pinning forces [2] the latter would decrease as predicted in Eq. 19 with α_y that would depend on the concentration of the oxygen vacancies. We acknowledge though that more data would be needed to draw

safer conclusion on a possible agreement between theory and experiments. For instance, the same type of experiments as those reported in Ref. [2] could be performed with irradiated samples to modify the number of pinning points.

References

1. Arsenault, R., Esterling, D.: Metall. Trans. A **20**, 1411 (1989)
2. Auslaender, O., Luan, L., Straver, E., Hoffman, J., Koshnick, N., Zeldov, E., Bonn, D., Liang, R., Hardy, W., Moler, K.: Nature **5**, 35 (2009)
3. Barabasi, A.L., Stanley, H.E.: Fractal Concepts in Surface Growth. Cambridge University Press, Cambridge (1995)
4. Blanter, Y.M., Vinokur, V.: Phys. Rev. B **66**, 132101 (2002)
5. Blatter, G., Feigelman, M., Geshkenbein, V., Larkin, A., Vinokur, V.: Rev. Mod. Phys. **66**, 1125 (1994)
6. Bouchaud, E.: J. Phys.: Condens. Matter **9**, 4319 (1997)
7. Brazovskii, S., Nattermann, T.: Adv. Phys. **53**, 177 (2004)
8. Chauve, P., Giamarchi, T., LeDoussal, P.: Phys. Rev. B **62**, 6241 (2000)
9. Curtin, W., Olmsted, D., Hector, L.: Nat. Mater. **5**, 875 (2006)
10. D'Anna, G., Benoit, W., Vinokur, V.: J. Appl. Phys. **82**, 5983 (1997)
11. Didenko, D.A., Pustovalov, V.: J. Low Temp. Phys. **11**, 65 (1973)
12. Fisher, D.: Phys. Rev. Lett. **56**, 1964 (1986)
13. Fleischer, R.: Acta Metall. **11**, 203 (1963)
14. Fleischer, R.: The Strengthening of Metals. Reinold Press Edition (1964), p. 93
15. Fleischer, R., Hibbard, W.: The Relation Between Structure and Mechanical Properties of Metals, vol. 1. H.M.S.O., London (1963), p. 262
16. Foreman, A., Makin, M.: Philos. Mag. **14**, 911 (1966)
17. Friedel, J.: Dislocations. Addison-Wesley, New York (1964), p. 224
18. Gennes, P.D., Matricon, J.: Rev. Mod. Phys. **36**, 45 (1964)
19. Hiratani, M., Bulatov, V.: Philos. Mag. Lett. **84**, 461 (2004)
20. Hirth, J., Lothe, J.: Theory of Dislocations. Wiley Interscience, New York (1982), p. 180
21. Joanny, J., de Gennes, P.: J. Chem. Phys. **81**, 552 (1984)
22. Kierfeld, J., Vinokur, V.: Phys. Rev. Lett. **96**, 175502 (2006)
23. Labusch, R.: Phys. Status Solidi **19**, 715 (1967)
24. Labusch, R.: Phys. Status Solidi **41**, 659 (1970)
25. Labusch, R.: Acta Metall. **20**, 917 (1972)
26. Larkin, A.: Sov. Phys. JETP **31**, 784 (1970)
27. Larkin, A., Ovchinnikov, Y.N.: J. Low Temp. Phys. **34**, 409 (1979)
28. Marian, J., Caro, A.: Phys. Rev. B **74**, 024113 (2006)
29. Moretti, P., Carmen-Miguel, M., Zaiser, M., Zapperi, S.: Phys. Rev. B **69**, 214103 (2004)
30. Mott, N.: Imperfections in Nearly Perfect Crystals. Wiley, New York (1952), p. 173
31. Mott, N., Nabarro, F.: Report on the Strength of Solids. Physical Society, London (1948), pp. 1–19
32. Nabarro, F.: Dislocations and Properties of Real Materials. The Institute of Metals, London (1985), p. 152
33. Narayan, O., Fisher, D.: Phys. Rev. B **48**, 7030 (1993)
34. Nogaret, T., Rodney, D.: Phys. Rev. B **74**, 134110 (2006)
35. Olmsted, D., Hector, L., Curtin, W., Clifton, R.: Model. Simul. Mater. Sci. Eng. **13**, 371 (2005)
36. Park, G., Cunningham, C., Cabrera, B., Huber, M.: Phys. Rev. B **68**, 1920 (1992)
37. Patinet, S., Proville, L.: Phys. Rev. B **78**, 104109 (2008)
38. Proville, L.: arXiv:0904.3357
39. Proville, L., Rodney, D., Bréchet, Y., Martin, G.: Philos. Mag. **86**, 3893 (2006)
40. Rodary, E., Rodney, D., Proville, L., Bréchet, Y., Martin, G.: Phys. Rev. B **70**, 054111 (2004)
41. Rosso, A., LeDoussal, P., Wiese, K.: Phys. Rev. B **75**, 220201 (2007)
42. Rusakov, V., Vasiliev, S., Chabanenko, V., Yurov, A., Nabialek, A., Piechota, S., Szymczak, H.: Acta Phys. Pol. A **109**, 641 (2006)
43. Suzuki, T., Takeuchi, S., Yoshinaga, H.: Dislocation Dynamics and Plasticity. Springer, Berlin (1991), p. 32
44. Tanguy, A., Vettorel, T.: Eur. Phys. J. B **38**, 71 (2004)
45. Tapasa, K., Bacon, D., Osetsky, Y.N.: Model. Simul. Mater. Sci. Eng. **14**, 1153 (2006)
46. Tapasa, K., Bacon, D., Osetsky, Y.N.: Acta Mater. **55**, 93 (2007)
47. Wiese, K.: Acta Phys. Slovaca **52**, 341 (2002)
48. Xu, Z., Picu, R.: Phys. Rev. B **76**, 94112 (2007)
49. Zapperi, S., Ciseau, P., Durin, G., Stanley, E.: Phys. Rev. B **58**, 6353 (1998)
50. Zapperi, S., Zaiser, M.: Mater. Sci. Eng. A **309–310**, 348 (2001)